Miner Petrol (2013) 107:591–608
DOI 10.1007/s00710-013-0285-3

ORIGINAL PAPER

Zircon U-Pb age, geochemical, and Sr-Nd-Pb isotopic constraints on the origin of alkaline intrusions in eastern Shandong Province, China

Shen Liu · Caixia Feng · Ruizhong Hu · Shan Gao · Tao Wang · Guangying Feng · Youqiang Qi · Ian M. Coulson · Shaocong Lai

Received: 12 June 2012 / Accepted: 13 March 2013 / Published online: 26 March 2013

Abstract Alkaline intrusions in the eastern Shandong Province consist of quartz monzonite and granite. U-Pb zircon ages, geochemical data, and Sr-Nd-Pb isotopic data for these rocks are reported in the present paper. Laser ablation inductively coupled plasma mass spectrometry (LA-ICP-MS) U-Pb zircon analyses yielded consistent ages ranging from 114.3±0.3 to 122.3±0.4 Ma for six samples of the felsic rocks. The felsic rocks are characterised by a wide range of chemical compositions (SiO_2=55.14–77.63 wt. %, MgO=0.09–4.64 wt. %, Fe_2O_3=0.56–7.6 wt. %, CaO=0.40–5.2 wt. %), light rare earth elements (LREEs) and large ion lithophile elements (LILEs) (i.e., Rb, Pb, U) enrichment, as well as significant rare earth elements (HREEs) and heavy field strength (HFSEs) (Nb, Ta, P and Ti) depletion, various and high $(^{87}Sr/^{86}Sr)_i$ ranging from 0.7066 to 0.7087, low ε_{Nd} (t) values from −14.1 to −17.1, high neodymium model ages (T_{DM1}=1.56–2.38Ga, T_{DM2}=2.02–2.25Ga), $^{206}Pb/^{204}Pb$= 17.12–17.16, $^{207}Pb/^{204}Pb$=15.44–15.51, and $^{208}Pb/^{204}Pb$= 37.55–37.72. The results suggested that these rocks were derived from an enriched crustal source. In addition, the alkaline rocks also evolved as the result of the fractionation of potassium feldspar, plagioclase, +/− ilmenite or rutile and apatite. However, the alkaline rocks were not affected by crustal contamination. Moreover, the generation of the alkaline rocks can be attributed to the structural collapse of the Sulu organic belt due to various processes.

Editorial handling: J. G. Raith

S. Liu (✉) · C. Feng · S. Lai
State Key Laboratory of Continental Dynamics
and Department of Geology, Northwest University,
Xi' an 710069, China
e-mail: liushen@vip.gyig.ac.cn

S. Liu
e-mail: liushen@nwu.edu.cn

R. Hu · G. Feng · Y. Qi
State Key Laboratory of Ore Deposit Geochemistry,
Institute of Geochemistry, Chinese Academy of Sciences,
Guiyang 550002, China

S. Gao
State Key Laboratory of Geological Processes and Mineral
Resources, China University of Geosciences,
Wuhan 430074, China

T. Wang
Chengdu University of Technology,
Chengdu 610059, China

I. M. Coulson
Solid Earth Studies Laboratory, Department of Geology,
University of Regina,
Regina, Saskatchewan S4S 0A2, Canada

Introduction

In the vicinities of Rizhao, Qingdao, and Weihai occur a wide range of lithologies that include volcanic, intrusive and metamorphic rocks (Ye et al. 1996; Cong 1996; Jahn et al. 1996; Zhao et al. 1997; Zhou and Lu 2000; Fan et al. 2001; Hong et al. 2003; Zheng et al. 2003; Guo et al. 2004; Huang et al. 2005; Yang et al. 2005a, b).

The intrusive rocks are represented by gabbro, granitoids, diorite, alkaline rocks, mafic dykes (Guo et al. 2004; Yang et al. 2005a, b; Liu et al. 2008a, b), as well as adakites (Guo et al. 2006), that are widely distributed throughout eastern Shandong Province. These rocks, and in particular, the alkaline rocks (Guo et al. 2005; Yang et al. 2005a, b; Liu et al. 2008a, b), contain valuable information concerning deep geodynamic processes and, as such, can be used to study the orogenic processes of continental subduction and the role of crust-mantle interaction in this part of China (Menzies and Kyle 1972; Jahn et al. 1996; Ye et al. 2000; Fan et al. 2001; Guo et al. 2004).

Alkaline rocks are generally thought to have their origins within the upper mantle (Ren 2003). These rocks are common in anorogenic, intraplate extensional, and/or rift-related tectonic settings (Currie 1970; Coulson 2003; Goodenough et al. 2003). However, alkaline rocks may also be generated during late to post-orogenic stages of magmatism (Coulson et al. 1999), such as in the Permian-Triassic Western Mediterranean Province (Bonin et al. 1987), the Pan-African Arabian Shield (Harris 1985), the Himalayas (Turner et al. 1996; Miller et al. 1999; Williams et al. 2004), Sulu belts (Yang et al. 2005a, b; Liu et al. 2008a, b), and others (Sylvester 1989; Guo et al. 2005). Felsic alkaline rocks (e.g., monzonite, syenite, and A-type granite) are also commonly intimately associated with alkaline mafic rocks (e.g., mafic dykes), especially alkali to transitional basalts (Upton et al. 2003; Yang et al. 2005a, b). As such, alkaline rocks require detailed investigation, particularly the alkaline associations within the eastern Shandong Province that are poorly understood. At present, only two alkaline associations have been reported upon in this part of China, namely, the Jiazishan and Junan-Wulian complexes, which are exposed in the eastern Shandong Province (Jiaodong) (Lin et al. 1992; Yang et al. 2005a, b; Liu et al. 2008a, b). The origin of these rocks remains controversial (i.e., they are formed as the result of slab break-off, post-orogenic extension, and foundering of lower crust) (Yang et al. 2005a, b; Xie et al. 2006; Liu et al. 2008a, b). The work of our group on ~110–120 Ma alkaline intrusions may provide further constraints in this debate, and as a result aid in determining the petrogenetic processes that occurred at a late evolutionary stage. Laser ablation inductively coupled plasma mass spectrometry (LA-ICP-MS) U-Pb geochronology, major and trace element geochemistry, as well as Sr-Nd-Pb isotope data from the younger alkaline associations of quartz-monzonite-A-type granite that formed in an extensional setting (Fig. 1) in the eastern Shandong Province are presented in this study. These data have been used to discuss the petrogenesis of the investigated alkaline associations.

Geological setting and petrography

Jiaodong is generally divided into two metamorphic terrains along the east northeast-trending Wulian-Qingdao-Rongcheng Fault. The south terrain is a high-pressure, blueschist unit, and the north one is an associated unit consisting of ultra-high pressure (UHP) metamorphic granitic gneiss, granulite and subordinate eclogite, schist, amphibolite, marble, as well as quartzite (Cao et al. 1990; Zhai et al. 2000; Guo et al. 2004). Mesozoic igneous rocks are widely distributed in Jiaodong, and mainly formed between 225 Ma and 114 Ma (Zhao et al. 1997; Zhou and Lu 2000; Fan et al. 2001; Zhou et al. 2003; Guo et al. 2004, 2006, 2005; Huang et al. 2005; Meng et al. 2005; Yang et al. 2005a, b). The study area dealt within the present paper is located in the eastern section of Shandong Province near to the city of Jiaonan (Fig. 1). Alkaline associations of quartz-monzonite (JS-1 and 2, DGZ1-1, 2, and 3) and syenogranite (ZZS1, 4; DCZ-1, 2, and 4; CQY1-1 and 5; CQY2-2 and 7; CQY3-2 and 3; as well as YZS-1 and 4) from this area were investigated (Fig. 1). Some mafic dykes appear within these felsic intrusions. Each suite is described in the following subsections.

Quartz-monzonite

Quartz-monzonite intrudes into Archaean or Lower Proterozoic gneiss (Fig. 1). The light grey-coloured monzonite is medium-to coarse-grained with granular and porphyritic textures. It has a composition of 36–45 % subhedral orthoclase and 8–15 % quartz, 30–35 % euhedral andesine, as well as 8–12 % diopside and 3.0–5.0 % biotite and amphibole. Accessory minerals include apatite, zircon, magnetite, and titanite.

Syenogranite

Syenogranite also mainly intrudes into the Archaean or Lower Proterozoic gneiss (Fig. 1). It is commonly light grey to pink, with a composition of 30–35 % quartz, 25–40 % perthite, 16–20 % albite ($An_{0\text{-}5.0}$), and minor muscovite. Accessory minerals include zircon, magnetite, and apatite.

Analytical procedures

U-Pb dating by the LA-ICP-MS method

Zircon was separated from six samples (JS01, DGZ01, ZZS02, DCZ01, CQY01, and YZS01) using conventional heavy liquid and magnetic techniques at the Langfang Regional Geological Survey, Hebei Province, China. Zircon separates were examined under transmitted and reflected light, as well as by cathodoluminescence petrography at the State Key Laboratory of Continental Dynamics, Northwest University, China to observe their external and internal structures. Laser-ablation techniques were employed for zircon age determinations (Table 1; Figs. 2 and 3) using an Agilent 7500a ICP-MS instrument equipped with a 193 nm excimer laser at the State Key Laboratory of Geological Processes and Mineral Resources, China University of

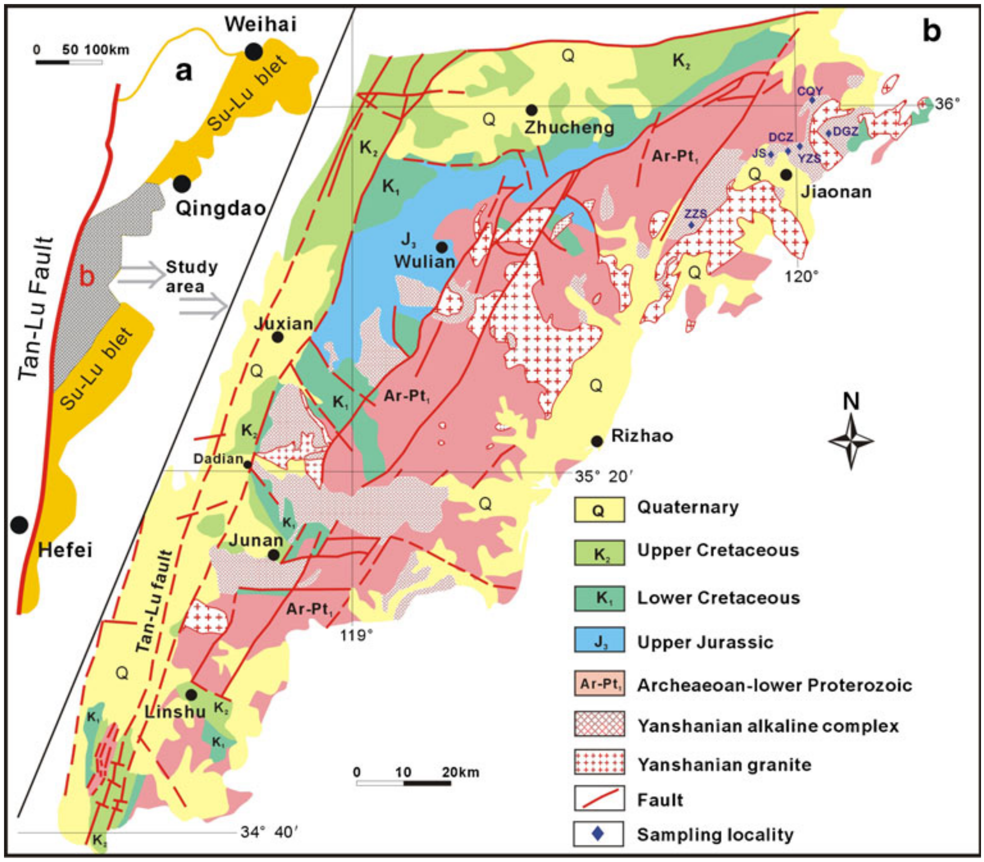

Fig. 1 **a** Simplified tectonic map of the Sulu Belt, eastern China (modified after Guo et al. 2004). **b** Geological map of the study areas showing the distributions of the alkaline intrusions (modified after BGMRS 1991)

Geoscience, Wuhan, China. Zircon # 91500 was used as a standard, and NIST 610 was used to optimise the results. A spot diameter of 24 μm was used. Prior to LA-ICP-MS zircon U-Pb dating, the surfaces of the grain mounts were washed in dilute HNO_3 and pure alcohol to remove any potential lead contamination. The analytical methodology has been described in detail by Yuan et al. (2004) and Liu et al. (2010). Correction for common Pb was performed following Andersen (2002). Data were processed using the GLITTER and ISOPLOT programs (Ludwig 2003) (Table 1; Fig. 3). Errors for individual analyses by LA-ICP-MS were quoted at the 95 % (1σ) confidence level.

Major elemental, trace elemental and isotopic analyses

Nineteen samples were collected to carry out major and trace element determinations as well as Sr-Nd-Pb isotopic analyses. Whole-rock samples were trimmed to remove altered surfaces, cleaned with deionised water, and then crushed and powdered using an agate mill. Major elements were analysed using a PANalytical Axios-advance (Axios PW4400) X-ray fluorescence spectrometer (XRF) at the State Key Laboratory of Ore Deposit Geochemistry, Institute of Geochemistry, Chinese Academy of Sciences. Fused glass discs were used and the analytical precision was better than 5 %, as determined based on the Chinese National standards: GSR-1 and GSR-3 (Table 2). Loss on ignition (LOI) was obtained using 1 g of powder heated to 1,100 °C for 1 h. Trace elements were analysed by plasma optical emission MS and ICP-MS at the National Research Center of Geo-analysis, Chinese Academy of Geosciences following procedures described by Qi et al. (2000). The discrepancy among triplicates was less than 5 % for all elements. Analysis results of the international standards OU-6 and GBPG-1 were in agreement with the recommended values (Table 3).

For the analyses of Rb-Sr and Sm-Nd isotopes, sample powders were spiked with mixed isotope tracers, dissolved in Teflon capsules with $HF+HNO_3$ acids, and separated by conventional cation-exchange techniques. Isotopic measurements were performed using a Finnigan Triton Ti thermal ionization mass spectrometer at the State Key Laboratory of Geological Processes and Mineral Resources, China University of Geosciences, Wuhan, China. Procedural blanks were <200 pg for Sm and Nd, as well as <500 pg for Rb and Sr. Mass fractionation corrections for Sr and Nd isotopic ratios were based on $^{86}Sr/^{88}Sr=0.1194$ and $^{146}Nd/^{144}Nd=0.7219$, respectively. Analyses of standards yielded the following results: NBS987 gave $^{87}Sr/^{86}Sr=0.710246\pm16$ (2σ) and La Jolla gave $^{143}Nd/^{144}Nd=0.511863\pm8$ (2σ). Pb was separated and purified by conventional cation-exchange technique (AG1×8, 200–400 resin) with diluted HBr as

Table 1 LA-ICPMS U-Pb isotopic data for zircons from the alkaline rocks in Jiaodong, Shandong Province, China

	Isotopic ratios										Age(Ma)					
Spot	Th(ppm)	U(ppm)	Pb(ppm)	Th/U	$^{207}Pb/^{206}Pb$	1σ	$^{207}Pb/^{235}U$	1σ	$^{206}Pb/^{238}U$	1σ	$^{207}Pb/^{206}Pb$	1σ	$^{207}Pb/^{235}U$	1σ	$^{206}Pb/^{238}U$	1σ
JS01																
1	139	116	2.89	1.20	0.0545	0.0032	0.1289	0.0083	0.0190	0.0003	393	103	132	7	121	2
2	216	157	4.16	1.38	0.0529	0.0028	0.1265	0.0052	0.0190	0.0002	325	94	130	6	122	1
3	204	150	3.95	1.36	0.0542	0.0028	0.1315	0.0031	0.0192	0.0003	378	91	134	6	123	2
4	453	242	7.02	1.87	0.0494	0.0028	0.1275	0.0045	0.0192	0.0002	166	99	122	6	122	1
5	710	279	9.30	2.55	0.0504	0.0049	0.1236	0.0028	0.0192	0.0003	215	220	127	11	123	2
6	173	148	3.61	1.17	0.0516	0.0055	0.1242	0.0062	0.0189	0.0003	268	245	128	13	120	2
7	401	231	6.59	1.74	0.0490	0.0024	0.1230	0.0051	0.0193	0.0002	146	91	124	6	123	1
8	119	74.2	2.10	1.60	0.0534	0.0072	0.1240	0.0065	0.0190	0.0004	346	304	133	17	121	2
9	178	111	3.06	1.60	0.0512	0.0059	0.1221	0.0042	0.0187	0.0003	251	259	126	13	119	2
10	144	97.7	2.63	1.48	0.0569	0.0059	0.1247	0.0072	0.0188	0.0003	487	237	133	13	120	2
11	90.7	72.1	1.79	1.26	0.0575	0.0033	0.1246	0.0036	0.0186	0.0003	512	87	134	7	119	2
DGZ01																
1	1047	1036	23.3	1.01	0.0559	0.0041	0.1219	0.0059	0.0184	0.0004	450	115	120	8	115	3
2	97.7	70.6	1.73	1.38	0.0499	0.0028	0.1184	0.0076	0.0184	0.0002	188	99	114	6	117	2
3	433	196	5.44	2.21	0.0461	0.0031	0.1179	0.0068	0.0185	0.0003	149	109	7	120	2	
4	440	138	4.91	3.18	0.0484	0.0013	0.1209	0.0082	0.0184	0.0002	117	43	118	3	119	1
5	845	300	8.94	2.82	0.0518	0.0025	0.1210	0.0079	0.0184	0.0002	277	83	121	5	120	2
6	404	200	5.56	2.02	0.0504	0.0026	0.1206	0.0081	0.0183	0.0002	213	99	116	6	114	1
7	506	205	6.06	2.47	0.0511	0.0022	0.1186	0.0065	0.0184	0.0002	247	80	115	5	113	1
8	80.3	56.9	1.40	1.41	0.0503	0.0072	0.1193	0.0095	0.0184	0.0004	211	294	110	15	112	3
9	78.5	67.5	1.52	1.16	0.0557	0.0084	0.1191	0.0057	0.0186	0.0004	440	337	120	17	117	2
10	139	94	2.20	1.48	0.0488	0.0042	0.1202	0.0083	0.0185	0.0003	137	196	116	9	120	2
11	134	125	2.95	1.06	0.0527	0.0055	0.1211	0.0074	0.0184	0.0003	316	191	119	12	116	3
12	133	85	2.23	1.57	0.0482	0.0014	0.1188	0.0082	0.0184	0.0002	110	50	110	3	119	0.9
ZZS02																
1	435	372	9.64	1.17	0.0461	0.0024	0.1185	0.0038	0.0179	0.0002	5	111	113	5	117	1
2	400	512	11.4	0.78	0.0493	0.0017	0.1214	0.0041	0.0178	0.0002	161	59	120	4	117	1
3	1052	1091	24.9	0.96	0.0485	0.0012	0.1213	0.0042	0.0179	0.0001	123	43	116	3	116	0.9
4	166	240	5.35	0.69	0.0473	0.0032	0.1195	0.0047	0.0178	0.0002	66	148	115	7	118	2
5	4779	4129	97.5	1.16	0.0478	0.0007	0.1193	0.0021	0.0179	0.0001	91	23	114	2	117	0.7
6	1798	1065	29.2	1.69	0.0497	0.0029	0.1189	0.0036	0.0179	0.0002	182	134	114	6	111	1
7	156	133	3.05	1.17	0.0564	0.0047	0.1215	0.0024	0.0179	0.0003	467	129	120	8	108	2
8	1483	1606	35.4	0.92	0.0502	0.0010	0.1196	0.0035	0.0179	0.0001	203	33	115	2	111	0.8

Table 1 (continued)

	Isotopic ratios										Age(Ma)					
Spot	Th(ppm)	U(ppm)	Pb(ppm)	Th/U	$^{207}Pb/^{206}Pb$	1σ	$^{207}Pb/^{235}U$	1σ	$^{206}Pb/^{238}U$	1σ	$^{207}Pb/^{206}Pb$	1σ	$^{207}Pb/^{235}U$	1σ	$^{206}Pb/^{238}U$	1σ
9	1935	1006	28.1	1.92	0.0482	0.0011	0.1186	0.0032	0.0178	0.0001	110	41	114	2	115	0.8
10	1060	689	16.9	1.54	0.0504	0.0014	0.1202	0.0028	0.0181	0.0002	211	52	115	3	115	1
11	761	793	17.7	0.96	0.0496	0.0013	0.1210	0.0031	0.0178	0.0002	175	46	118	3	116	1
12	907	1064	23.5	0.85	0.0500	0.0037	0.1189	0.0034	0.0178	0.0002	193	168	113	8	112	1
13	1095	1036	23.5	1.06	0.0505	0.0012	0.1217	0.0026	0.0179	0.0001	216	41	119	3	114	0.9
DCZ02																
1	42.7	35.4	0.90	1.20	0.0591	0.0110	0.1201	0.0078	0.0185	0.0006	649	401	144	24	116	4
2	200	113	3.39	1.76	0.0577	0.0071	0.1203	0.0095	0.0184	0.0005	272	292	143	16	117	3
3	57.6	45.6	1.16	1.26	0.0587	0.0087	0.1200	0.0067	0.0185	0.0005	556	332	142	19	116	3
4	99.8	51.2	1.56	1.95	0.0586	0.0094	0.1202	0.0095	0.0183	0.0005	750	329	145	21	118	3
5	236	118	3.46	2.00	0.0585	0.0032	0.1203	0.0083	0.0185	0.0003	340	113	143	7	118	2
6	142	77.8	2.28	1.83	0.0595	0.0035	0.1204	0.0096	0.0183	0.0003	656	87	146	8	118	2
7	83.0	59.2	1.58	1.40	0.0586	0.0081	0.1204	0.0086	0.0185	0.0005	553	315	142	18	118	3
8	83.5	66.5	1.71	1.26	0.0590	0.0041	0.1203	0.0076	0.0186	0.0004	607	114	143	9	119	2
9	162	95.9	2.83	1.69	0.0584	0.0043	0.1201	0.0095	0.0184	0.0004	118	161	144	10	118	2
CQY01																
1	601	413	10.9	1.46	0.0487	0.0018	0.1296	0.0048	0.0192	0.0002	133	71	124	4	123	1
2	586	484	11.9	1.21	0.0496	0.0015	0.1291	0.0029	0.0189	0.0002	175	54	123	4	121	1
3	381	370	8.79	1.03	0.0453	0.0017	0.1234	0.0044	0.0193	0.0002	−7	55	115	4	123	1
4	779	654	16.3	1.19	0.0477	0.0013	0.1216	0.0032	0.0191	0.0002	82	48	120	3	122	1
5	451	364	9.07	1.24	0.0492	0.0021	0.1305	0.0059	0.0193	0.0002	155	85	125	5	123	1
6	555	494	12.2	1.12	0.0486	0.0015	0.1303	0.0039	0.0195	0.0002	126	55	124	4	124	1
7	436	405	9.86	1.08	0.0464	0.0019	0.1229	0.0025	0.0193	0.0002	17	64	118	4	123	1
8	213	226	5.23	0.94	0.0492	0.0021	0.1276	0.0053	0.0189	0.0002	158	74	122	5	121	1
9	1653	1199	30.0	1.38	0.0486	0.0010	0.1279	0.0025	0.0190	0.0002	129	36	122	3	121	1
YZS01																
1	103	107	2.53	0.97	0.0517	0.0048	0.1296	0.0078	0.0186	0.0003	272	211	126	11	121	2
2	160	154	3.74	1.03	0.0569	0.0029	0.1293	0.0083	0.0192	0.0003	488	82	142	7	122	2
3	293	281	6.78	1.04	0.0575	0.0032	0.1291	0.0084	0.0191	0.0002	76	76	138	5	119	1
4	96.6	98.5	2.36	0.98	0.0545	0.0034	0.1290	0.0078	0.0192	0.0004	392	104	136	8	120	2
5	101	99.3	2.43	1.02	0.0584	0.0038	0.1291	0.0078	0.0190	0.0003	545	95	143	9	119	3
6	119	123	2.93	0.97	0.0540	0.0034	0.1290	0.0080	0.0189	0.0004	373	111	133	8	123	2
7	267	181	4.88	1.47	0.0572	0.0042	0.1301	0.0079	0.0192	0.0003	499	119	138	9	121	2
8	95.9	97.7	2.32	0.98	0.0574	0.0035	0.1300	0.0082	0.0189	0.0003	505	93	137	7	122	2

Table 1 (continued)

Spot	Isotopic ratios Th(ppm)	U(ppm)	Pb(ppm)	Th/U	$^{207}Pb/^{206}Pb$	1σ	$^{207}Pb/^{235}U$	1σ	$^{206}Pb/^{238}U$	1σ	Age(Ma) $^{207}Pb/^{206}Pb$	1σ	$^{207}Pb/^{235}U$	1σ	$^{206}Pb/^{238}U$	1σ
9	100	103	2.48	0.97	0.0568	0.0055	0.1301	0.0082	0.0187	0.0003	484	218	138	12	119	2
10	106	100	2.38	1.05	0.0583	0.0033	0.1290	0.0080	0.0191	0.0003	290	111	141	7	121	2
11	209	163	3.94	1.28	0.0581	0.0035	0.1291	0.0083	0.0190	0.0002	230	90	142	5	118	1
12	193	158	4.09	1.22	0.0530	0.0030	0.1304	0.0086	0.0192	0.0003	330	101	132	7	121	2
13	114	110	2.75	1.04	0.0546	0.0027	0.1292	0.0078	0.0197	0.0003	397	80	137	6	123	2
14	118	118	2.75	1.00	0.0518	0.0057	0.1290	0.0080	0.0186	0.0003	277	250	127	13	119	2

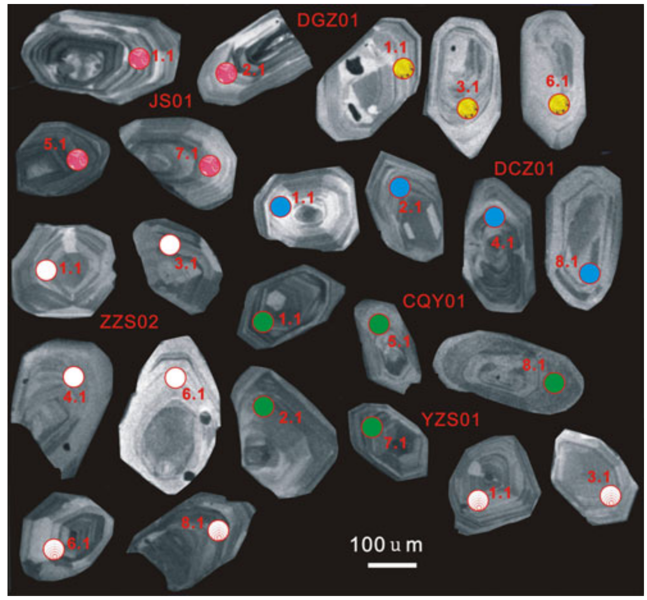

Fig. 2 Selected zircon cathodoluminescenc CL images of alkaline rocks in the eastern Shandong Province

eluant. Procedural blanks were <50 pg for Pb. Analyses of NBS981 during the period of analysis yielded $^{204}Pb/^{206}Pb$=0.0896±15, $^{207}Pb/^{206}Pb$=0.9145±8, and $^{208}Pb/^{206}Pb$=2.162±2. Total procedural Pb blanks were in the range of 0.1–0.3 ng. The analytical results for Sr-Nd-Pb isotopes are presented in Table 4.

Results

Zircon U-Pb ages

Euhedral zircon grains in samples JS01, DGZ01, ZZS02, DCZ01, CQY01, and YZS01 are clean and prismatic, with magmatic oscillatory zoning (Fig. 3). A total of 11 grains have a weighted mean $^{206}Pb/^{238}U$ age of 121±0.5 Ma (1σ) (95 % confidence interval) for JS01 (Table 1; Fig. 3a), 9 grains have a weighted mean $^{206}Pb/^{238}U$ age of 118±0.4 Ma (1σ) (95 % confidence interval) for DGZ01 (Table 1; Fig. 3b), 13 grains have a weighted mean $^{206}Pb/^{238}U$ age of 114±0.3 Ma (1σ) (95 % confidence interval) for ZZS02 (Table 1; Fig. 3c), 12 grains have a weighted mean $^{206}Pb/^{238}U$ age of 118±0.8 Ma (1σ) (95 % confidence interval) for DCZ01 (Table 1; Fig. 3d), 9 grains have a weighted mean $^{206}Pb/^{238}U$ age of 122±0.4 Ma (1σ) (95 % confidence interval) for CQY01 (Table 1; Fig. 3e), and 14 grains have a weighted mean $^{206}Pb/^{238}U$ age of 122±0.5 Ma (1σ) (95 % confidence interval) for YZS01 (Table 1; Fig. 3f). These determinations are the best estimates of the crystallisation ages of the alkaline rocks. There was also no inherited zircon characteristic observed.

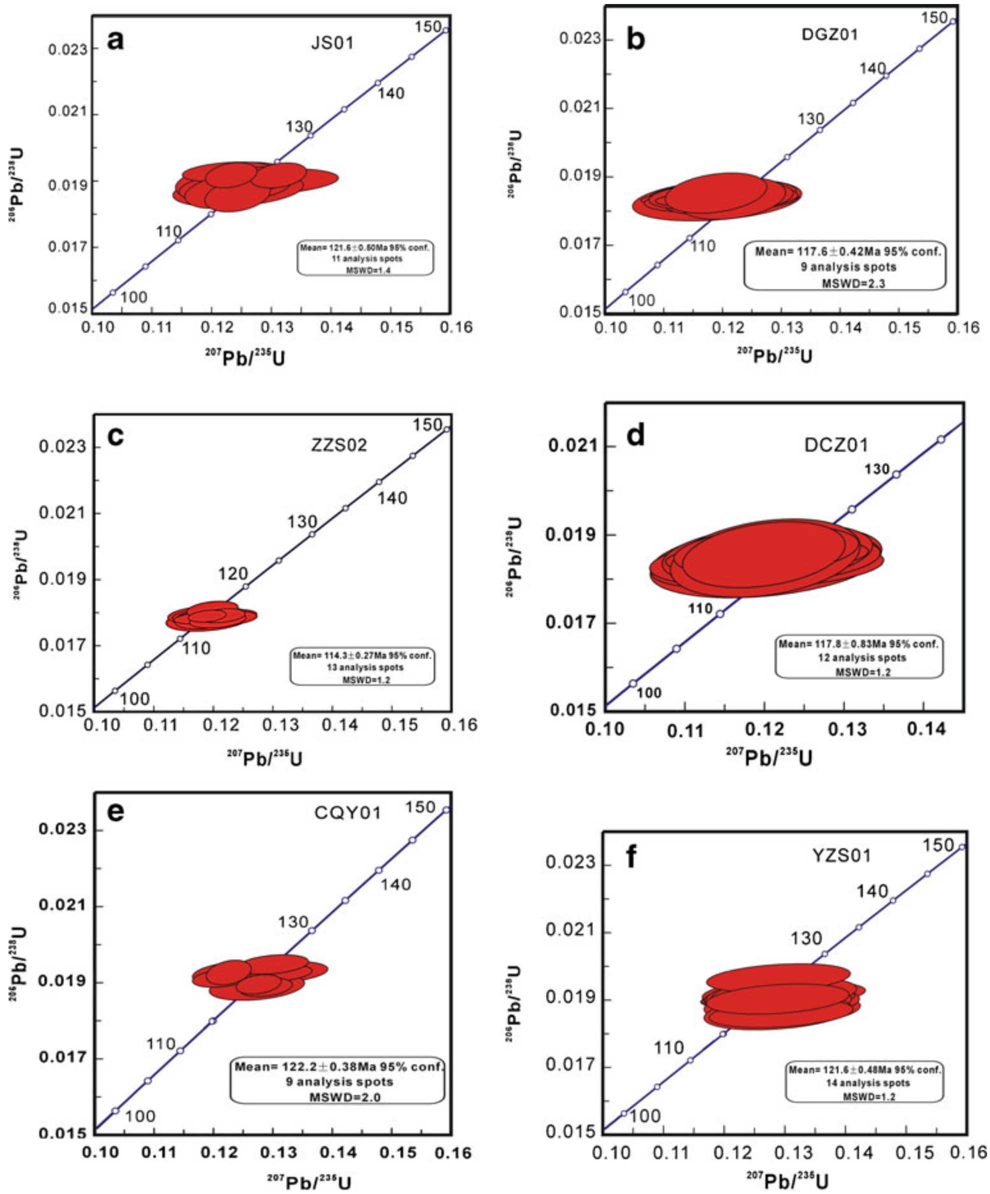

Fig. 3 LA-ICP-MS zircon U-Pb concordia diagrams for the investigated quartz monzonite, monzonite, and granite intrusions in the eastern Shandong Province

Major and trace elements

Geochemical data of the quartz monzonite and syenogranite intrusions in the study area are listed in Tables 2 and 3.

The quartz monzonite and granite samples have a wide range of chemical compositions, with SiO_2=55.14–77.63 wt.%, Al_2O_3=12.13–19.78 wt.%, MgO=0.09–4.64 wt. %, Fe_2O_3=0.56–7.61 wt. %, and CaO=0.40–4.84 wt. %. They are relatively high in total alkalis, with K_2O=3.74–4.85 wt. % and Na_2O=3.71–4.64 wt. %, and total K_2O+Na_2O ranging from 8.21 to 8.99 wt. %. All felsic rocks lie in the alkaline field when plotted on the total alkali-silica (TAS) diagram (Fig. 4a). All samples also straddle the shoshonitic series in the Na_2O vs. K_2O plot (Fig. 4b). In a plot of the molar ratios of Al_2O_3/(Na_2O+K_2O) versus Al_2O_3/ (CaO+Na_2O+K_2O), the rocks are mostly metaluminous, except for some samples falling along the boundary of the metaluminous and peralkaline fields (Fig. 4c). The analysed quartz monzonite and syenogranite samples display regular trends of decreasing TiO_2, Al_2O_3, Fe_2O_3, MgO, CaO, Na_2O, P_2O_5, Sr, Zr, Ba, Cr, and Ni, increasing SiO_2, as well as positive correlations between K_2O, Rb, and SiO_2 (Fig. 5 and the figures not shown). The 10,000×Ga/Al ratios of the monzonite and granite samples range from 1.84 to 3.04. In the Ga/Al vs. Zr discrimination diagram of Whalen et al. (1987), the alkaline rocks are all classified as A-type granite.

The quartz monzonite and syenogranite intrusions are characterised by LREE enrichment and HREE depletion, with a wide range in $(La/Yb)_N$ values (6.36–43.6) and Eu/Eu* (0.2–1.4) (Table 3 and Fig. 6a). On average, quartz monzonite has a higher Eu/Eu*(1.1–1.4) than the granite (0.2–0.98). In primitive mantle-normalised trace element

Table 2 Major oxides (wt. %) for the alkaline rocks in Jiaodong, Shandong Province, China

Sample	Rock type	SiO_2	Al_2O_3	Fe_2O_3	MgO	CaO	Na_2O	K_2O	MnO	P_2O_5	TiO_2	LOI	Total	$Mg^{\#}$	T_{Zr}(°C)	Na_2O+K_2O
JS-1	Quartz monzonite	59.0	19.5	4.80	1.73	4.84	4.50	3.90	0.07	0.35	0.71	1.07	100.51	44	836	8.40
JS-2		60.0	19.8	4.32	1.45	4.69	4.64	3.85	0.06	0.28	0.63	0.55	100.27	42	835	8.49
DGZ1-1	Quartz monzonite	56.2	15.5	7.41	4.41	4.71	4.56	3.74	0.10	0.52	1.27	2.36	100.71	57	829	8.30
DGZ1-2		55.8	15.4	7.47	4.51	4.70	4.58	3.75	0.11	0.51	1.25	2.33	100.43	57	829	8.33
DGZ1-3		55.1	15.4	7.61	4.64	5.20	4.64	3.77	0.11	0.52	1.28	2.59	100.91	57	825	8.41
ZZS-1	Syenogranite	75.8	12.4	0.84	0.09	0.40	4.11	4.54	0.04	0.02	0.11	0.31	98.65	19	846	8.65
ZZS-4		76.1	12.3	0.97	0.10	0.42	3.89	4.54	0.04	0.03	0.12	0.77	99.29	18	847	8.43
DCZ-1	Syenogranite	67.7	15.4	3.11	1.32	2.39	4.23	4.34	0.05	0.18	0.48	0.54	99.67	48	885	8.57
DCZ-2		67.2	15.1	3.21	1.28	2.42	4.25	4.17	0.06	0.18	0.49	0.23	98.57	47	892	8.42
DCZ-4		65.7	14.9	2.92	1.21	2.21	4.49	4.21	0.05	0.18	0.47	3.29	99.66	49	875	8.70
CQY1-1	Syenogranite	77.2	12.1	0.63	0.41	0.54	4.41	4.81	0.04	0.02	0.14	0.30	100.62	59	751	9.21
CQY1-5		76.8	12.4	0.64	0.35	0.66	3.75	4.74	0.03	0.02	0.10	0.48	99.93	55	757	8.49
CQY2-2		77.6	12.3	0.68	0.23	0.68	3.86	4.64	0.04	0.02	0.11	0.44	100.64	43	752	8.49
CQY2-7		77.5	12.6	0.57	0.19	0.61	3.74	4.69	0.03	0.01	0.10	0.43	100.47	42	780	8.43
CQY3-2		76.7	12.4	0.62	0.10	0.52	4.25	4.75	0.03	0.02	0.11	0.51	100.05	26	794	8.99
CQY3-3		76.7	12.5	0.56	0.09	0.52	3.71	4.85	0.03	0.01	0.10	0.42	99.50	26	760	8.57
YZS-1	Syenogranite	65.4	15.0	4.43	1.91	3.19	3.92	4.47	0.07	0.24	0.56	1.07	100.29	49	840	8.39
YZS-4		66.9	14.7	4.01	1.79	3.08	3.82	4.57	0.07	0.23	0.55	0.69	100.39	50	819	8.39
YZS-6		66.9	14.7	3.84	1.69	3.07	3.95	4.48	0.06	0.22	0.55	0.69	100.10	49	823	8.43
GSR-3	RV*	44.64	13.83	13.4	7.77	8.81	3.38	2.32	0.17	0.95	2.37	2.24	99.88			
GSR-3	MV*	44.75	14.14	13.35	7.74	8.82	3.18	2.3	0.16	0.97	2.36	2.12	99.89			
GSR-1	RV*	72.83	13.4	2.14	0.42	1.55	3.13	5.01	0.06	0.09	0.29	0.7	99.62			
GSR-1	MV*	72.65	13.52	2.18	0.46	1.56	3.15	5.03	0.06	0.11	0.29	0.69	99.70			

LOI Loss on Ignition. $Mg^{\#}$=100*Mg/ (Mg+∑Fe) atomic ratio. "–": Not calculated. Note that T_{Zr} (°C) is calculated from zircon saturation thermometry (Watson and Harrison 1983). RV*: recommended values; MV*: measured values; The values for GSR-1 and GSR-3 from Wang et al. (2003)

Table 3 The trace elements composition (ppm) for the alkaline rocks in Jiaodong, Shandong Province, China

Sample	Sc	V	Cr	Ni	Rb	Sr	Y	Nb	Ba	Ga	La	Ce	Pr	Nd	Sm
JS-1	9.13	68.8	12.5	5.31	61.5	1348	15.6	9.77	3370	19.0	61.7	103	11.5	41.3	6.03
JS-2	11.8	85.4	12.3	5.34	57.4	1399	19.9	10.1	2453	20.4	73.2	116	12.9	46.5	7.04
DGZ1-1	15.8	135	132.4	68.2	95.9	710	21.4	18.3	1917	18.0	43.4	81.6	9.47	36.4	6.43
DGZ1-2	16.7	132	129.5	70.8	72.9	802	21.4	18.4	1917	17.7	43.0	82.7	9.45	36.8	6.40
DGZ1-3	17.3	137	137.3	73.4	64.5	761	21.6	18.3	1608	18.3	43.3	82.1	9.38	36.8	6.24
ZZS-1	8.91	6.81	0.71	0.74	239	29.7	25.5	54.2	96	19.1	22.4	38.0	3.88	13.0	2.72
ZZS-4	7.25	3.39	3.18	0.43	236	29.3	25.8	57.3	107	19.3	20.7	36.5	3.73	12.3	2.44
DCZ-1	7.66	60.1	22.9	11.5	90.9	509	19.2	13.3	1742	18.4	80.4	110	9.99	32.4	4.61
DCZ-2	10.5	57.6	30.2	25.9	79.5	558	21.9	13.8	1835	19.3	92.6	120	11.3	36.7	5.14
DCZ-4	9.22	59.8	24.0	13.1	65.8	497	19.5	14.0	1690	17.6	62.0	89.4	8.81	29.1	4.24
CQY1-1	4.06	7.26	6.56	3.04	190	39.7	5.42	17.1	62.9	18.6	25.3	39.1	3.05	7.98	1.06
CQY1-5	5.16	3.67	6.36	2.72	202	41.1	6.96	14.1	61.1	18.8	29.8	45.6	3.77	10.2	1.23
CQY2-2	4.52	3.67	18.3	8.27	175	37.5	7.38	16.1	70.9	19.8	29.1	44.5	3.82	10.4	1.23
CQY2-7	3.01	2.88	15.6	7.42	182	35.8	6.92	16.2	61.4	18.8	24.3	38.5	3.39	9.21	1.32
CQY3-2	5.29	3.92	7.46	3.66	203	43.5	8.44	14.6	91.0	19.0	31.4	48.2	4.12	11.5	1.49
CQY3-3	5.13	2.62	11.4	4.86	173	40.6	7.19	13.5	95.1	20.0	27.8	41.4	3.52	9.47	1.25
YZS-1	12.1	74.2	37.2	17.8	100	554	19.9	14.1	1410	17.7	59.5	106	10.9	38.8	6.05
YZS-4	12.5	71.1	46.9	20.6	99.7	542	18.8	14.4	1380	17.1	49.1	88.2	9.37	33.2	5.36
YZS-6	12.0	67.2	51.6	23.4	96.9	552	17.9	13.1	1430	16.9	54.5	95.1	9.60	33.8	5.25
OU-6(RV*)	22.1	129	70.8	39.8	120	131	27.4	14.8	477	24.3	33.0	74.4	7.80	29.0	5.92
OU-6(MV*)	21.6	131	73.5	42.5	122	136	26.2	15.3	486	26.5	33.1	78.0	8.09	30.6	5.99
GBPG-1(RV*)	13.9	96.5	181	59.6	56.2	364	18.0	9.93	908	18.6	53.0	103	11.5	43.3	6.79
GBPG-1(MV*)	14.2	103	187	60.6	61.4	377	17.2	8.74	921	20.9	51.0	105	11.6	42.4	6.63

Sample	Eu	Gd	Tb	Dy	Ho	Er	Tm	Yb	Lu	Hf	Zr	Ta	Pb	Th	U	δEu
JS-1	2.76	6.00	0.66	3.07	0.58	1.75	0.25	1.64	0.26	6.85	309	0.62	15.3	9.82	1.99	1.40
JS-2	2.42	6.26	0.75	3.73	0.70	2.06	0.29	1.86	0.28	4.59	299	0.66	14.2	9.51	1.66	1.11
DGZ1-1	2.01	6.15	0.81	4.02	0.79	2.23	0.29	2.01	0.28	5.24	323	1.19	6.89	3.42	0.74	0.98
DGZ1-2	1.99	5.84	0.77	4.06	0.79	2.16	0.28	1.86	0.28	5.34	321	1.20	5.98	3.45	0.75	1.00
DGZ1-3	1.97	5.82	0.76	4.10	0.79	2.11	0.30	1.94	0.28	5.28	324	1.13	6.43	3.27	0.75	1.00
ZZS-1	0.15	1.87	0.48	3.00	0.63	1.91	0.33	2.29	0.35	5.75	184	4.83	18.5	21.5	5.54	0.20
ZZS-4	0.16	1.80	0.43	2.90	0.61	1.95	0.34	2.34	0.35	5.48	165	4.64	20.4	20.9	5.25	0.23
DCZ-1	1.15	3.23	0.55	2.75	0.52	1.49	0.20	1.32	0.20	5.74	302	0.69	13.3	13.8	1.09	0.91
DCZ-2	1.23	3.59	0.61	3.06	0.59	1.64	0.23	1.62	0.25	6.07	319	0.70	13.8	15.1	1.04	0.87
DCZ-4	1.03	2.92	0.51	2.63	0.51	1.39	0.22	1.36	0.21	6.57	352	0.68	12.5	13.1	1.07	0.90
CQY1-1	0.17	0.80	0.12	0.63	0.16	0.58	0.10	0.91	0.16	3.64	66.7	1.44	27.4	24.4	2.55	0.56
CQY1-5	0.16	1.00	0.15	0.83	0.22	0.74	0.13	1.12	0.21	3.78	85.3	1.64	28.1	30.3	3.74	0.45
CQY2-2	0.18	1.08	0.17	0.87	0.24	0.81	0.15	1.17	0.23	3.05	63.5	1.67	28.3	29.0	4.28	0.48
CQY2-7	0.19	1.02	0.16	0.88	0.23	0.78	0.14	1.12	0.20	3.83	86.4	1.98	28.9	26.2	4.25	0.49

Table 3 (continued)

Sample	Eu	Gd	Tb	Dy	Ho	Er	Tm	Yb	Lu	Hf	Zr	Ta	Pb	Th	U	δEu
CQY3-2	0.21	1.12	0.19	1.06	0.26	0.86	0.15	1.27	0.24	4.52	101	1.96	28.3	29.4	6.48	0.49
CQY3-3	0.21	0.91	0.15	0.82	0.22	0.72	0.12	1.03	0.18	2.76	69.0	1.30	25.3	25.8	4.26	0.61
YZS-1	1.47	5.00	0.67	3.41	0.71	2.07	0.29	1.99	0.29	5.24	305	1.06	17.9	14.0	1.80	0.82
YZS-4	1.30	4.48	0.60	3.13	0.67	1.92	0.27	1.91	0.28	4.71	298	1.08	19.0	14.1	1.62	0.81
YZS-6	1.35	4.48	0.62	2.96	0.64	1.87	0.26	1.72	0.28	4.30	296	0.98	18.3	13.8	1.58	0.85
OU-6(RV*)	1.36	5.27	0.85	4.99	1.01	2.98	0.44	3.00	0.45	4.70	174	1.06	28.2	11.5	1.96	
OU-6(MV*)	1.35	5.50	0.83	5.06	1.02	3.07	0.45	3.09	0.47	4.86	183	1.02	32.7	13.9	2.19	
GBPG-1(RV*)	1.79	4.74	0.60	3.26	0.69	2.01	0.30	2.03	0.31	6.07	232	0.40	14.1	11.2	0.90	
GBPG-1(MV*)	1.69	4.47	0.59	3.17	0.66	2.02	0.29	2.031	0.31	5.93	224	0.46	14.5	11.4	0.99	

The values for GBPG-1 from Thompson et al. (2000), and for OU-6 from Potts and Kane (2005)

diagrams, quartz-monzonite and syenogranite samples show enrichment in LILEs (i.e., Rb, Pb, U, and sometimes Ba) and depletion in some Ba, Sr, and HFSEs (i.e., Nb, Ta, P, and Ti) (Fig. 6b).

Sr-Nd and Pb isotopes

Sr-Nd and Pb isotopic data have been obtained from (nineteen) representative quartz monzonite and syenogranite samples (Table 4). The alkaline rocks show very different $(^{87}Sr/^{86}Sr)_i$ values ranging from 0.7066 to 0.7087, a relatively large variation in ε_{Nd} (t) values from −14.1 to −17.1, and high neodymium model ages (T_{DM1}=1.56–2.38Ga, T_{DM2}=2.02–2.25Ga). These results suggest an enriched source region. The Sr-Nd isotopic compositions (Fig. 7) are also comparable to those of late Mesozoic volcanic rocks, alkaline rocks, granites granites and diorites, as well as adakites in Jiaodong (Zhao et al. 1997; Zhou and Lu 2000; Guo et al. 2006; Huang et al. 2005; Yang et al. 2005a, b; Liu et al. 2008a, b) (Fig. 7). The Pb isotopic ratios in the alkaline rocks are $^{206}Pb/^{204}Pb$=17.12–17.16, $^{207}Pb/^{204}Pb$= 15.44–15.52 and $^{208}Pb/^{204}Pb$=37.55–37.72, respectively. These ratios significantly differ from those from the Yangtze lithospheric mantle (Yan et al. 2003), and are identical to those of Jiaodong alkaline rocks, Jiazishan alkaline complex and mafic rocks from the central North China Craton, as well as to the Dabie Orogen (Zhang et al. 2004; Yan et al. 2003; Xie et al. 2006; Liu et al. 2008a, b), having a clear EM-1 affinity (Zindler and Hart 1986; Fig. 8a, b).

Discussion

Crustal contamination

Continued assimilation and fractional crystallisation (AFC), or magma mixing is usually postulated to explain the occurrence of co-magmatic felsic rocks (e.g., DePaolo 1981; Devey and Cox 1987; Marsh 1989; Mingram et al. 2000). AFC and magma mixing would result in a negative correlation between SiO_2 and ε_{Nd} (*t*) values, as well as a positive correlation between SiO_2 and $(^{87}Sr/^{86}Sr)_i$ ratios (Fig. 9). The absence of these characteristic features in the studied Jiaodong alkaline rocks,indicates that magma evolution was not significantly affected by crustal contamination or magma mixing. Further support for this is provided in the high and consistent neodymium model ages (T_{DM1}=1.56–2. 38 Ga, T_{DM2}=2.02–2.25 Ga) (Table 4). The geochemical and Sr-Nd-Pb isotopic signatures of the studied Jiaodong alkaline rocks are, therefore, interpreted to be mainly inherited from an enriched crusted source, as was shown in the Sr-Nd and Pb isotopic data.

Table 4 Sr-Nd-Pb isotopic compositions for the alkaline felsic rocks in Jiaodong, Shandong Province, China

Sample	Age (Ma)	Sm (ppm)	Nd (ppm)	Rb (ppm)	Sr (ppm)	$^{87}Rb/^{86}Sr$	$^{87}Sr/^{86}Sr$	2σ	$(^{87}Sr/^{86}Sr)_i$	$^{147}Sm/^{144}Nd$	$^{143}Nd/^{144}Nd$	2σ	$(^{143}Nd/^{144}Nd)_i$	$\varepsilon_{Nd}(t)$	T_{DM1} (Ga)	T_{DM2} (Ga)	$^{206}Pb/^{204}Pb$	$^{207}Pb/^{204}Pb$	$^{208}Pb/^{204}Pb$
JS-1	121.6	6.03	41.3	61.5	1348	0.1320	0.708300	10	0.708072	0.0882	0.511686	8	0.511616	−16.9	1.78	2.25	17.152	15.512	37.563
JS-2		7.04	46.5	57.4	1399	0.1186	0.708255	10	0.708050	0.0916	0.511707	8	0.511634	−16.5	1.80	2.22	17.153	15.513	37.565
DGZ1-1	117.6	6.43	36.4	95.9	710	0.3910	0.707447	10	0.706795	0.1069	0.511838	8	0.511756	−14.3	1.87	2.05	17.151	15.513	37.712
DGZ1-2		6.40	36.8	72.9	802	0.2633	0.707454	9	0.707015	0.1051	0.511831	9	0.511750	−14.4	1.85	2.06	17.121	15.485	37.714
DGZ1-3		6.24	36.8	64.5	761	0.2453	0.707890	12	0.707481	0.1025	0.511812	8	0.511733	−14.7	1.83	2.08	17.143	15.488	37.716
ZZS-1	114.3	2.72	13.0	239	29.7	23.32	0.746007	8	0.708093	0.1270	0.511793	8	0.511698	−15.5	2.38	2.17	17.154	15.506	37.657
ZZS-4		2.44	12.3	236	29.3	23.35	0.746181	12	0.708211	0.1197	0.511798	12	0.511709	−15.3	2.19	2.15	17.155	15.508	37.655
DCZ-1	117.8	4.61	32.4	90.9	509	0.5170	0.709354	12	0.708488	0.0862	0.511758	8	0.511692	−15.5	1.66	2.13	17.138	15.451	37.665
DCZ-2		5.14	36.7	79.5	558	0.4125	0.708148	10	0.707457	0.0848	0.511677	10	0.511612	−17.1	1.74	2.25	17.141	15.454	37.672
DCZ-4		4.24	29.1	65.8	497	0.3829	0.708310	8	0.707669	0.0880	0.511705	10	0.511637	−16.6	1.75	2.22	17.143	15.456	37.668
CQY1-1	122.2	1.06	7.98	190	39.7	13.850	0.732426	12	0.708352	0.0803	0.511684	12	0.511620	−16.8	1.67	2.23	17.152	15.523	37.643
CQY1-5		1.23	10.2	202	41.1	14.224	0.732993	12	0.708270	0.0729	0.511708	10	0.511650	−16.2	1.56	2.17	17.142	15.522	37.645
CQY2-2		1.23	10.4	175	37.5	13.505	0.732148	10	0.708673	0.0715	0.511677	8	0.511620	−16.8	1.58	2.22	17.143	15.511	37.647
CQY2-7		1.32	9.21	182	35.8	14.713	0.734310	8	0.708737	0.0866	0.511705	10	0.511636	−16.5	1.73	2.21	17.151	15.513	37.648
CQY3-2		1.49	11.5	203	43.5	13.505	0.732105	10	0.708630	0.0783	0.511716	9	0.511653	−16.1	1.61	2.18	17.145	15.487	37.651
CQY3-3		1.25	9.47	173	40.6	12.332	0.728017	8	0.706583	0.0798	0.511691	9	0.511627	−16.7	1.66	2.22	17.142	15.491	37.654
YZS-1	121.6	6.05	38.8	100	554	0.5224	0.708482	10	0.707580	0.0943	0.511837	8	0.511764	−14.1	1.67	2.02	17.146	15.436	37.546
YZS-4		5.36	33.2	99.7	542	0.5323	0.708442	8	0.707523	0.0976	0.511779	10	0.511704	−15.3	1.80	2.12	17.143	15.435	37.563
YZS-6		5.25	33.8	96.9	552	0.5080	0.708605	9	0.707728	0.0939	0.511708	8	0.511636	−16.6	1.83	2.23	17.145	15.441	37.558

Chondrite Uniform Reservoir (CHUR) values ($^{87}Rb/^{86}Sr$=0.0847, $^{87}Sr/^{86}Sr$=0.7045, $^{147}Sm/^{144}Nd$=0.1967 $^{143}Nd/^{144}Nd$=0.512638) are used for the calculation. $\lambda_{Rb}=1.42\times10^{-11}$ year^{-1} (Steiger and Jäger 1977); $\lambda_{Sm}=6.54\times10^{-12}$ year^{-1} (Lugmair and Harti 1978)

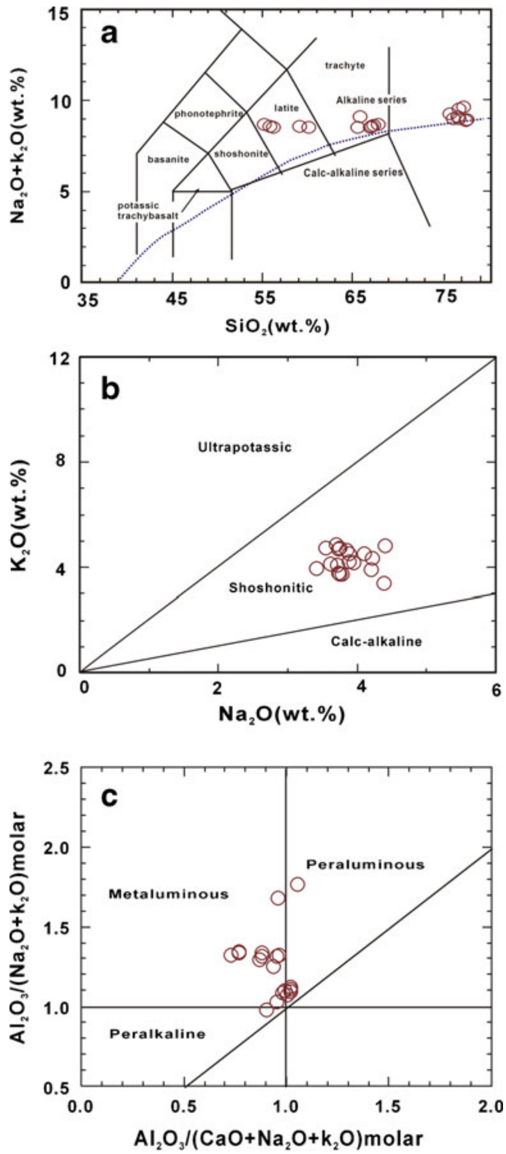

Fig. 4 Classification of the monzonite and granite intrusions from eastern Shandong Province based on three diagrams. **a** TAS diagram. All major elemental data have been recalculated to 100 % on a LOI-free basis (after Middlemost 1994; Le Maitre 2002). **b** K_2O vs. Na_2O diagram. The alkaline association is shown to be shoshonitic (after Middlemost 1990). **c** $Al_2O_3/(Na_2O+K_2O)$ molar vs. $Al_2O_3/(CaO+Na_2O+K_2O)$ molar plot. Most samples fall in the metaluminous field, but some samples straddle the metaluminous and peralkaline field boundary

Fractional crystallisation

For the studied felsic samples, SiO_2 shows a negative correlation with TiO_2, Al_2O_3, Fe_2O_3, MgO, CaO, Na_2O, and P_2O_5 (Fig. 5a–f and h). This may relate to the fractionation of clinopyroxene, hornblende, plagioclase, Ti-bearing phases (ilmenite, titanite, etc.), and apatite. The negative Nb, Ta, and Ti anomalies exhibited in all the investigated alkaline rocks (Fig. 6a) also agree with the fractionation of Fe-Ti oxides, such as ilmenite and titanite. However, parallel rare earth elements (REEs) distribution patterns, coupled with high SiO_2 contents in some of the investigated samples (e.g., ZZS-1, ZZS-4, CQY1-1, CQY1-5, CQY2-2, CQY2-7, CQY3-2, and CQY3-3) require alternative explanations. Nevertheless, the negative Ba, Sr, and Eu anomalies shown by many rocks (Fig. 6a and b) imply the fractionation of potassium feldspar and plagioclase.

Jiaodong alkaline rocks exhibit continuously decreasing Zr with increasing SiO_2. This result indicates that zircon was saturated in the magma, which was also controlled by fractional crystallisation (Li et al. 2007). Zircon saturation thermometry (Watson and Harrison 1983) provides a simple and robust means of estimating magma temperatures from bulk-rock compositions. The calculated effects of fractional crystallisation are shown in the mineral vector diagrams presented as Fig. 10a and b. The alkaline rocks (the granite samples, in particular) display a combined vector of potassium feldspar and plagioclase fractionation in Fig. 10a. On the other hand, Fig. 10b shows that potassium feldspar fractionation is more important than plagioclase in controlling Ba abundance. The calculated zircon saturation temperatures (T_{Zr}) of the alkaline rocks lie in the range 751–892 °C (Table 2), which represents the crystallisation temperature of the magma. The syenogranite samples (CQY type) show much lower T_{Zr} values (751–794 °C) than the other rocks (819–892 °C) (Table 2).

Petrogenesis

Above all, the geochemical signatures of the alkaline rocks favor their derivation from silicic- rather than basaltic magmas. In other words, the studied rocks were derived from an enriched crustal source (Liu and Xu 2011). Additional support for this explanation comes from high-pressure experimental work that has demonstrated that granite and quartz monzonite cannot result directly from the partial melting of mantle peridotite (Colling 1982; Pitcher 1984).

A Proterozoic stratum in the Jiaodong peninsula is composed dominantly of biotite schist, biotite plagioclase gneiss, amphibolite, granulite, and minor slate and marble. In addition, the alkaline rocks are characterized by negative Eu anomalies and low HREE concentrations (Fig. 6a, b), which could indicate a garnet-bearing source. The Sr-Nd and Pb isotopic compositions of the alkaline rocks differ from those of the North China and Yangtze Cratons (Jahn et al. 1999; Li 2007), implying that the source of the studied rocks was neither the North China nor the Yangtze Craton alone. One possibility is that the source may have been a mixture of materials from both cratons. We use the whole-rock two-stage Nd model ages to infer the possible age of the source. The two-stage Nd model ages (T_{DM2}=2.02–2.25 Ga)

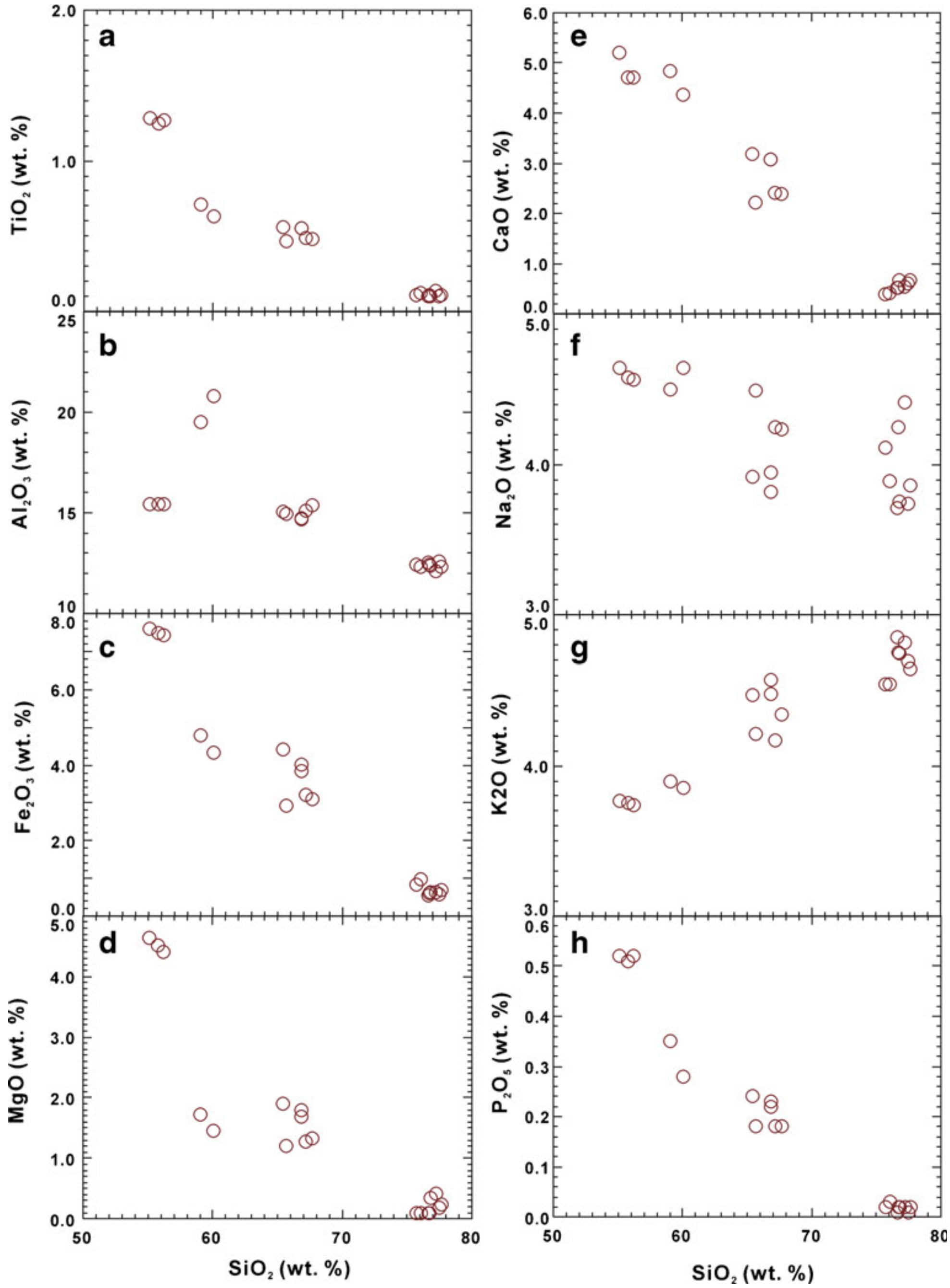

Fig. 5 Selected variation diagrams of major elemental oxides vs. SiO_2 plots for the alkaline felsic rocks in eastern Shandong Province

suggest the presence of an Early Proterozoic crustal component in the source of the studied rocks.

At present, there compete various petrogenetic models for the generation of alkaline felsic rocks (e.g., syenite and A-type granite) (Yang et al. 2005a, b; Zhong et al. 2007; Liu et al. 2008a, b), such as (1) partial melting of lower-crustal rocks under the fluxing of volatiles, (2) fractionation of mantle-derived magmas with or without crustal contamination, (3) mixing of basic and silicic melts and their differentiates, as well as, (4) partial melting of an enriched lithospheric mantle beneath an orogenic belt, due to hybridisation of melts derived from foundered lower crustal eclogite. Among them, the insignificant variations in Sr-Nd isotopes with SiO_2 for the alkaline rocks (Fig. 9a, b) preclude the possibility of assimilation process in their genesis. Fractionation of mantle-derived magma without the interaction of crustal rocks, therefore, is proposed as the best model to explain the origin of the studied quartz monzonite and syenogranite intrusions. However, high-pressure experiments have demonstrated that granite cannot be formed through the partial melting of mantle peridotite. Hence, an alternative explanation must be sought for the generation of the investigated alkaline lithologies.

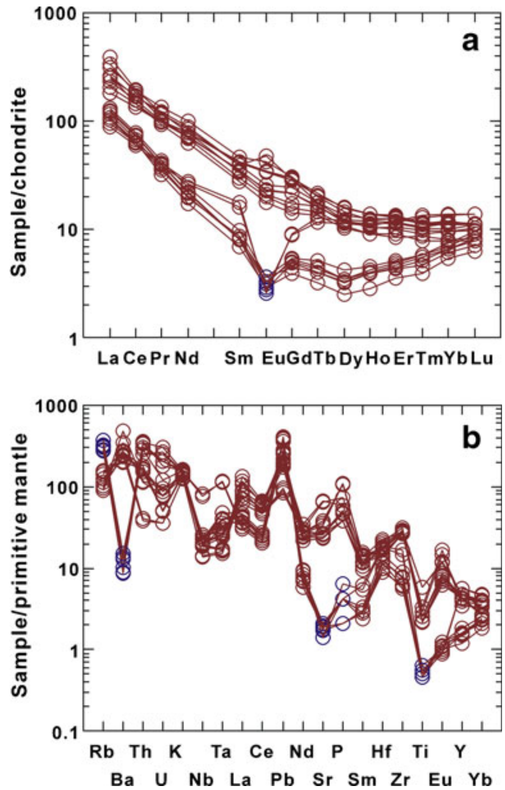

Fig. 6 Chondrite-normalised rare earth elements (REEs) diagrams and primitive mantle-normalised incompatible element distribution diagrams for the quartz monzonite, monzonite and granite intrusions in eastern Shandong Province. The normalisation values are from Sun and McDonough (1989)

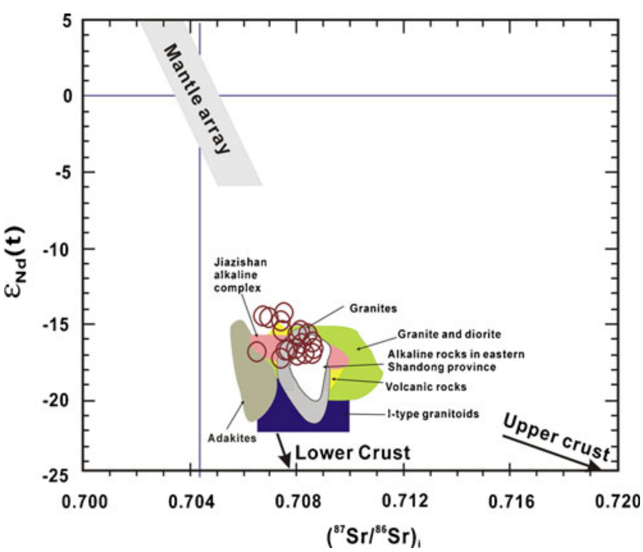

Fig. 7 Initial $^{87}Sr/^{86}Sr$ vs. $\varepsilon_{Nd}(t)$ diagram for the felsic rocks in eastern Shandong Province. Other igneous rocks from the Sulu Belt are also plotted for comparison: volcanic rocks from Fan et al. (2001) and Guo et al. (2004), Jiazishan alkaline Complex from Yang et al. (2005a), granites from Yang et al. (2005b), granite and diorite from Huang et al. (2005), adakites from Guo et al. (2006), I-type granitoids from Zhao et al. (1997) and Zhou and Lu (2000), as well as alkaline rocks in eastern Shandong Province from Liu et al. (2008a, b)

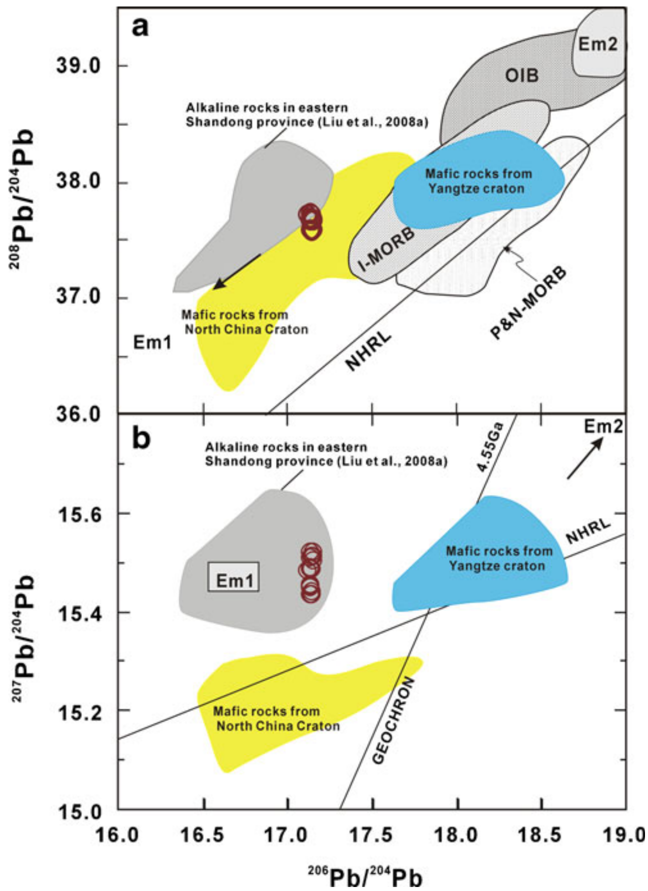

Fig. 8 $^{208}Pb/^{204}Pb$ and $^{207}Pb/^{204}Pb$ vs. $^{206}Pb/^{204}Pb$ diagrams for the studied alkaline felsic rocks, compared with Early Cretaceous mafic rocks from the North China and Yangtze Craton as well as alkaline rocks in eastern Shandong Province. Fields for Indian MORB and Pacific and North Atlantic MORB, OIB, NHRL, as well as 4.55 Ga geochron are from Barry and Kent (1988), Zou et al. (2000), and Hart (1984), respectively. Data on North China Craton are from Zhang et al. 2004 and Xie et al. (2006), Yangtze mafic rocks are from Yan et al. (2003); the alkaline rocks in eastern Shandong Province are from Liu et al. (2008a, b)

Field geology and petrographic observations can provide direct evidence in the recognition of magma mixing and, therefore, important clues for mantle-crust mixing (Mo et al. 2002; Wang et al. 2002; Shao et al. 2006). Generally, in the case of alkaline rocks, evidence for magma mixing includes bimodal plagioclase phenocryst populations, quenched enclaves, reverse zoning in clinopyroxene occurring within xenocrysts, gabbroic and dioritic dyke swarms, etc. These features, however, are lacking in the studied rocks. Moreover, there are no visible linear relationships identified between SiO_2, K_2O, Na_2O, CaO, Fe_2O_3 and MgO, in addition, the compositional variation in MgO and FeO lie off the magma mixing trend line (not shown). Collectively, this evidence clearly demonstrates that magma mixing did not play a role in the formation of the alkaline rocks (Zorpi et al. 1989). Additional support for this is provided in the

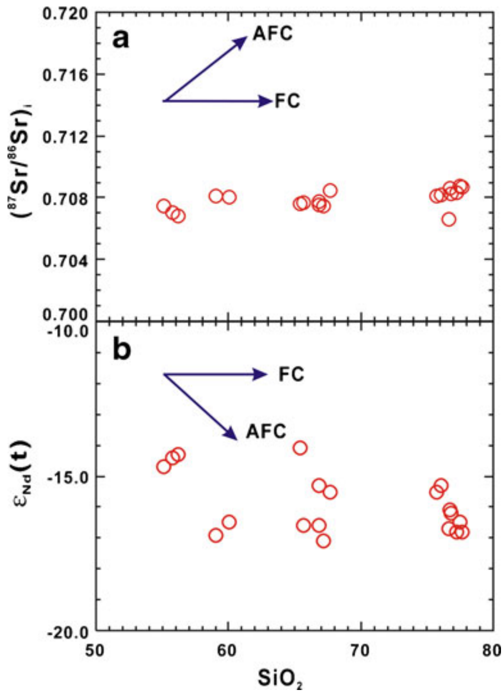

Fig. 9 Plots of: **a** initial $^{87}Sr/^{86}Sr$ ratio and **b** ε_{Nd} (t) value versus SiO_2 for the alkaline rocks from eastern Shandong Province, indicating crystal fractionation trends. *FC* fractional crystallisation; *AFC* assimilation and fractional crystallisation

consistent Nb/Ta ratios of our studied samples. In summary, the alkaline rocks studied in this paper were not derived through the mixing of mafic and silicic melts.

In the primitive mantle normalised diagrams illustrated in Fig. 6b, all the investigated rocks show very distinctive negative anomalies for HFSEs (e.g., Nb, Ta and Ti), suggesting involvement of components from ancient continental crust (Zhang et al. 2005). This reasoning is further supported by the low ε_{Nd} (t) values (−15.3 to −17.1) and high $(^{87}Sr/^{86}Sr)_i$ (0.7074–0.7088) of the studied rocks (Table 4; Fig. 7). Moreover, the fractional crystallization of minerals (principally plagioclase) suggests that the primary magma is hardly a mafic one. Hence, we still need to understand the petrogenetic process responsible for the generation of the eastern Shandong Province alkaline rocks.

Alkaline rocks are usually generated in post-collision extensional settings (Bonin et al. 1998; Yang et al. 2005a, b; Oyhantçabal et al. 2007), intra-plate rifts or deep faults (Burke et al. 2003; Ridolfi et al. 2006; Jung et al. 2007; Shellnutt and Zhou 2008), or by mantle plumes (Mchone 1996; Karmalkar et al. 2005; Srivastava et al. 2005). Based upon the discussion of source and the geological setting, we propose that the studied alkaline rocks were formed in an extensional / collapse tectonic setting.

The high-ultra high pressure metamorphic rocks of the Dabie-Sulu orogenic belt formed in response to the subduction, collision and exhumation of the Yangtze Craton relative to the North China Craton (NCC) (Wang et al. 1995; Cong 1996). In Early Triassic times (200–230 Ma), the collision of the Yangtze Craton under the NCC resulted in the formation of the Sulu orogenic. Susequent exhumation of Yangtze continental crust helped to form the Sulu Mélange zone; the resulting high- to ultra high-pressure lithotectonic assemblages (eclogite, garnet peridotite and granulite, etc.) and a deep-seated ductile deformation zone occurs right across the Jiaodong and Shandong province of China (Han 2000). After a prolonged period of sustainable and balanced stress, during the Late Jurassic, the stress field transformed into an extensional state; a piedmont depression developed as the Jiao-Lai basin with deposition of sediments (Lai-yang sediments, Han 2000). Late in the Early Cretaceous, the intensity of crustal extension increased resulting in the development of peculiar NE-trending shoshonitic dykes within the Jiaodong Peninsula, eastern Shandong Province, China. In the Late Cretaceous, as a result of continued extension of the basin (e.g., the Jiao-Lai basin), the subduction of the Pacific plate (Chen et al. 2004; Qiu et al. 2008; Yang et al. 2012) led to structural collapse of the Sulu organic belt (Zhao and Zheng 2009). As a result of this collapse, the lower part of the Sulu Mélange zone underwent partial melting, leading to the emplacement of the multiple and diverse magmas, that are represented in the study area as alkaline rocks (Han 2000).

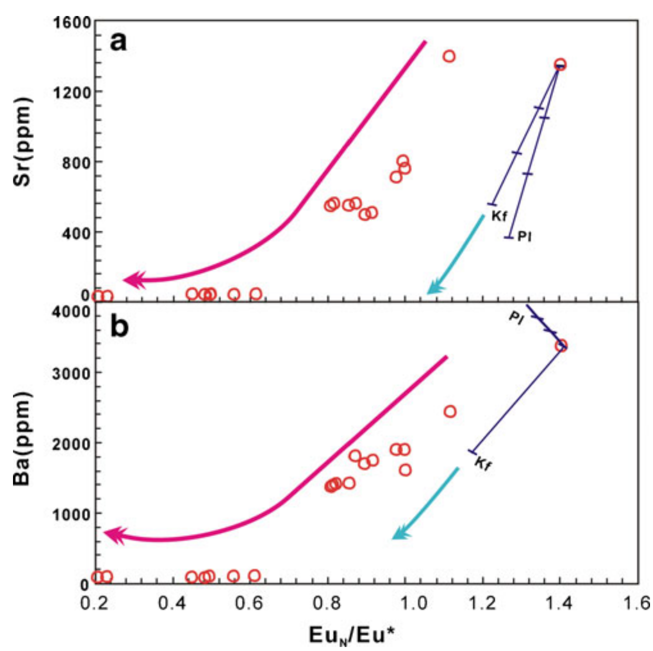

Fig. 10 Plots of Eu/Eu* vs.: **a** Sr and **b** Ba for the alkaline rocks. Mineral fractionation vectors were calculated using partition coefficients from Philpotts and Schnetzler (1970) and Bacon and Druit (1988). *Tick marks* indicate percentage of mineral phase removed in 10 % intervals; Pl-plagioclase, Kf-potassium feldspar

Conclusions

Based upon geochronological, geochemical, and Sr-Nd and Pb isotopic studies, the following conclusions can be drawn:

(1) LA-ICP-MS U-Pb zircon dating results indicates that the studied alkaline quartz monzonite and syenogranite intrusions formed between 114.3±0.3 and 122.3±0.4 Ma.
(2) The investigated alkaline rocks derived from an enriched source. The parental magma originated through partial melting of an enriched crust beneath the eastern Shandong Province. The possible fractionation of potassium feldspar and plagioclase resulted in an alkaline association with negligible crustal contamination. Zircon saturation temperatures (T_{Zr}) of the felsic rocks lie in the range 751–892 °C, which approximately represents the crystallisation temperatures of the magma.
(3) The alkaline rocks were produced due to partial melting of an enriched crust source due to the collapse of Sulu organic belt in response to the action of various processes such as extension of the Jiao-Lai basin, subduction of the Pacific plate and the exhumation of Yangtze Craton.

Acknowledgments The present research was supported by the Knowledge Innovation Project (KZCX2-YW-111-03), the opening project (08LCD08) of State Key Laboratory of Continental Dynamics, and the National Nature Science Foundation of China (40972071, 40634020). The authors gratefully acknowledge Lian Zhou for helping with Sr, Nd, and Pb isotope analyses and thank Yongsheng Liu and Zhaochu Hu for their help with LA-ICP-MS zircon U-Pb dating, as well as Prof. Guochun Zhao for editing the English.

References

Andersen T (2002) Correction of common lead in U-Pb analyses that do not report ^{204}Pb. Chem Geol 192:59–79
Bacon CR, Druit TH (1988) Compositional evolution of the zoned calcalkaline magma chamber of Mount-Mazama, Crater Lake, Oregon. Contrib Mineral Petrol 98:224–256
Barry TL, Kent RW (1988) Cenozoic magmatism in Mongolia and the origin of central and East Asian basalts. In: Flower MFJ, Chung SL, Lo CH, Lee TY (eds) Mantle dynamics and plate interactions in East Asia. American Geophysical Union-Geodynamics Series 27:347–364
Bonin B, Platevoet B, Vialette Y (1987) The geodynamic significance of alkaline magmatism in the Western Mediterranean compared with West Africa. In: Bowden P, Kinnaird J (eds) African Geology Reviews. Geological Journal 22:361–387
Bonin B, Azzouni-Sekkal A, Bussy F, Ferrag S (1998) Alkali-calcic and alkaline postorogenic (PO) granite magmatism: petrologic constraints and geodynamic settings. Lithos 45:45–70
Bureau of Geology and Mineral Resources of Shandong Province (BGMRS) (1991) Attached map 2 of regional geology of Shandong Province. Geological Publishing House, Beijing, in Chinese
Burke K, Ashwal LD, Webb SJ (2003) New way to map old sutures using deformed alkaline rocks and carbonatites. Geology 31:391–394
Cao G, Wang Z, Zhang C (1990) The Jiaonan terrane in Shandong Province and the tectonic significance of Wulian-Rongcheng fault. Shandong Geol 6:1–15 (in Chinese)
Chen B, Jahn BM, Arakaw Y, Zhai MG (2004) Petrogenesis of the Mesozoic intrusive complexes from the southern Taihang Orogen, North China Craton and Sr-Nd-Pb isotopic constraints. Contrib Mineral Petrol 148:489–501
Colling WJ (1982) Nature and origin of the A-the granite with particular reference to southearst Australia. Contrib Mineral Petrol 80:198–200
Cong BL (1996) Ultrahigh-pressure metamorphic rocks in the Dabie-Sulu Region of China. Science Press, Beijing: China and Kluwer Academic Publishing, Dordrecht 224
Coulson IM (2003) Evolution of the North Qôroq centre nepheline syenites, South Greenland: alkali-mafic silicates and the role of metasomatism. Mineral Mag 67:873–892
Coulson IM, Russell JK, Dipple GM (1999) Origins of the Zippa Mountain pluton: a Late Triassic, arc-derived, ultrapotassic magma from the Canadian Cordillera. Can J Earth Sci 36:1415–1434
Currie KL (1970) An hypothesis on the origin of alkaline rocks suggested by the tectonic setting of the Monteregian Hills. Can Mineral 10:411–420
DePaolo DJ (1981) Trace element and isotopic effects of combinedwallrock assimilation and fractionation crystallization. Earth Planet Sci Lett 53:189–202
Devey CW, Cox KG (1987) Relationships between crustal contamination and crystallization in continental flood basalt magmas with special reference to the Deccan Traps of the Western Ghats, India. Earth Planet Sci Lett 84:59–68
Fan WM, Guo F, Wang YJ, Lin G, Zhang M (2001) Postorogenic bimodal volcanism along the Sulu orogenic belt in eastern China. Phys Chem Earth A 26:733–746
Goodenough KM, Coulson IM, Wall F (2003) Intraplate alkaline magmatism: mineralogy and petrogenesis. Mineral Mag 67:829–830
Guo F, Fan WM, Wang YJ, Zhang M (2004) Origin of early Cretaceous calc-alkaline lamprophyres from the Sulu orogen in eastern China: implications for enrichment processes beneath continental collisional belt. Lithos 78:291–305
Guo JH, Chen FK, Zhang XM, Siebel W, Zhai MG (2005) Evolution of syn-to post-collisional magmatism from north Sulu UHP belt, eastern China: zircon U-Pb geochronology. Acta Petrol Sin 21:1281–1301
Guo F, Fan WM, Li CW (2006) Geochemistry of late Mesozoic adakites from the Sulu belt, eastern China: magma genesis and implications for crustal recycling beneath continental collisional orogens. Geol Mag 143:1–13
Han ZZ (2000) Characteristics and structure-forming background of Shandong-Jiangsu alkalic rock suite. Shandong Geol 16:5–10
Harris NBW (1985) Alkaline complexes from the Arabian Shield. In: Black R, Bowden P (eds) Alkaline Ring Complexes in Africa. J African Earth Sci 3:3–88
Hart SR (1984) A large-scale isotope anomaly in the Southern Hemisphere mantle. Nature 309:753–757
Hong DW, Wang T, Tong Y, Wang XX (2003) Mesozoic granitoids from North China Block and Qinling-Dabie-Sulu orogenic belt and their deep dynamic process. Earth Sci Front 10:231–256
Huang J, Zheng YF, Wu YB, Zhao ZF (2005) Geochemistry of elements and isotopes in igneous rocks from the Wulian region in the Sulu orogen. Acta Petrol Sin 21:545–568

Jahn BM, Cornichet J, Cong BL, Yui TF (1996) Ultrahigh-εNd eclogites from an ultrahigh-pressure metamorphic terrane of China. Chem Geol 127:61–79

Jahn BM, Wu FY, Lo CH, Tsai CH (1999) Crust-mantle interaction induced by deep subduction of the continental crust; geochemical and Sr-Nd isotopic evidence from post-collisional mafic-ultramafic intrusions of the Northern Dabie complex, central China. Chem Geol 157:119–146

Jung S, Hoffer E, Hoernes S (2007) Neo-Proterozoic rift-related syenites (Northern Damara Belt, Namibia): geochemical and Nd–Sr–Pb–O isotope constraints for mantle sources and petrogenesis. Lithos 96:415–435

Karmalkar NR, Rege S, Griffin WL, O'Reilly SY (2005) Alkaline magmatism from Kutch, NW India: implications for plume-lithosphere interaction. Lithos 81:101–119

Le Maitre RW (2002) Igneous rocks: a classification and glossary of terms, (2nd). Cambridge University Press, Cambridge, p 236

Li QZ (2007) The Pb-Sr-Nd isotopic characters of early Cretaceous mafic rocks in eastern China: the contribution of lower crust regarding mantle source. P.h. d dissertation. University of Science and Technology of China

Li XH, Li ZX, Li WX, Liu Y, Yuan C, Wei GJ, Qi CS (2007) U-Pb zircon, geochemical and Sr-Nd-Hf isotopic constraints on age and origin of Jurassic I- and A-type granites from central Guangdong, SE China: A major igneous event in response to foundering of a subducted flat-slab? Lithos 96:186–204

Lin JQ, Tan DJ, Chi XG, Bi LJ, Xie CF, Xu WL (1992) Mesozoic granites in Jiao-Liao Peninsula. Science Press, Beijing, p 208 (in Chinese with English abstract)

Liu L, Xu XS (2011) Genesis of the tianzhushan intermediate-felsic rocks from the Dabie Orogen and its geological significance. Geol J China Univ 17:137–150

Liu S, Hu R, Gao S, Feng C, Qi Y, Wang T, Feng G, Coulson IM (2008a) U-Pb zircon age, geochemical and Sr-Nd-Pb-Hf isotopic constraints on age and origin of alkaline intrusions and associated mafic dikes from Sulu orogenic belt, Eastern China. Lithos 106:365–379

Liu S, Hu RZ, Feng CX, Zou HB, Li C, Chi XG, Peng JT, Zhong H, Qi L, Qi YQ, Wang T (2008b) Cenozoic high Sr/Y volcanic rocks in the Qiangtang terrane, northern Tibet: geochemical and isotopic evidence for the origin of delaminated lower continental melts. Geol Mag 145:463–474

Liu YS, Hu ZC, Zong KQ, Gao CG, Gao S, Xu J, Chen HH (2010) Reappraisement and refinement of zircon U-Pb isotope and trace element analyses by LA-ICP-MS. Chin Sci Bull 55:1535–1546

Ludwig KR (2003) User's manual for isoplot/ex, version 3.00. A geochronological toolkit for microsoft excel: Berkeley Geochronology Center Special Publication 4:1–70

Lugmair GW, Harti K (1978) Lunar initial $^{143}Nd/^{144}Nd$: differential evolution of the lunar crust and mantle. Earth Planet Sci Lett 39:349–357

Marsh JS (1989) Geochemical constraints on coupled assimilation and fractional crystallization involving upper crustal compositions and continental tholeiitic magma. Earth Planet Sci Lett 92:78–80

Mchone JG (1996) Constraints on the mantle plume model for Mesozoic alkaline intrusions in northeastern North America. Can Mineral 34:325–334

Meng FC, Xue HM, Li TF, Yang HR, Liu FL (2005) Enriched characteristics of Late Mesozoic mantle under the Sulu orogenic belt: geochemical evidence from gabbro in Rushan. Acta Petrol Sin 21:1583–1592 (in Chinese with English abstract)

Menzies MA, Kyle PR (1972) Continental volcanism: a crust-mantle probe. In: Menzies MA (ed) Continental mantle. Oxford University Press, Oxford, pp 157–177

Middlemost EAK (1990) A simple classification of volcanic rocks. Bull Volcanol 36:382–397

Middlemost EAK (1994) Naming materials in the magma/igneous rock system. Earth Sci Rev 74:193–227

Miller C, Schuster R, Klötzli U, Frank W, Purtscheller F (1999) Post-collisional potassic and ultrapotassic magmatism in SW Tibet: geochemical and Sr-Nd-Pb-O isotopic constraints for mantle source characteristics and petrogenesis. J Petrol 40:1399–1424

Mingram B, Trumbull RB, Littman S, Gertenberger H (2000) A petrogenetic study of anorogenic felsic magmatism in the Cretaceous Paresis ring complex, Namibia: evidence for mixing of crust and mantle-derived components. Lithos 54:1–22

Mo XX, Luo ZH, Xiao QH (2002) Cognition and research methods of magma mixing for granite. Geological publishing House 53–63

Oyhantçabal P, Siegesmund S, Wemmer K, Frei R, Layer P (2007) Post-collisional transition from calc-alkaline to alkaline magmatism during transcurrent deformation in the southernmost Dom Feliciano Belt (Braziliano-Pan-African, Uruguay). Lithos 98:141–159

Philpotts JA, Schnetzler CC (1970) Phenocryst-matrix partition coefficients for K, Rb, Sr and Ba, with applications to anorthosite and basalt genesis. Geochim Cosmochim Acta 34:307–322

Pitcher WS (1984) (Translated by Tang LJ), type and environment of transform of granite. Geol Sci Technol Foreign 3:1–28

Potts PJ, Kane JS (2005) International association of geoanalysts certificate of analysis: certified reference material OU-6 (Penrhyn slate). Geostand Geoanal Res 29:233–236

Qi L, Hu J, Grégoire DC (2000) Determination of trace elements in granites by inductively coupled plasma mass spectrometry. Talanta 51:507–513

Qiu LG, Renm FL, Caom ZX, Zhang YQ (2008) Late Mesozoic magmatic activities and their constraints on geotectonic of Jiaodong Region. Geotecton Metallog 32:117–123

Ren KX (2003) Study progress of the alkaline rocks: a review. Geol Chem Miner 25:151–163 (in Chinese with English abstract)

Ridolfi F, Renzulli A, Macdonald R, Upton BGJ (2006) Peralkaline syenite autoliths from Kilombe volcano, Kenya Rift Valley: evidence for subvolcanic interaction with carbonatitic fluids. Lithos 91:373–392

Shao JA, Lu FX, Zhang LQ, Yang JH (2006) Discovery of xenocrysts in basalts of Yixian Formation in west Liaoning Province and its significance. Acta Petrol Sin 21:1547–1558 (in Chinese with English abstract)

Shellnutt JG, Zhou MF (2008) Permian, rifting related fayalite syenite in the Panxi region, SW China. Lithos 101:54–73

Srivastava RK, Heaman LM, Sinha AK, Shihua S (2005) Emplacement age and isotope geochemistry of Sung Valley alkaline–carbonatite complex, Shillong Plateau, northeastern India: implications for primary carbonate melt and genesis of the associated silicate rocks. Lithos 81:33–54

Steiger RH, Jäger E (1977) Subcommission on geochronology; convention on the use of decay constants in geochronology and cosmochronology. Earth Planet Sci Lett 36:359–362

Sun SS, McDonough WF (1989) Chemical and isotopic systematics of oceanic basalts: implications for mantle composition and processes. In: Saunders AD, Norry MJ (eds) Magmatism in the ocean basins. Geological Society Special Publication, London, pp 313–345

Sylvester PJ (1989) Post-collisional alkaline granites. J Geol 97:261–280

Thompson M, Potts PJ, Kane JS, Wilson S (2000) An international proficiency test for analytical geochemistry laboratories-report on round 5 (August 1999). Geostand Geoanal Res 24:E1–E28

Turner S, Arnaud N, Liu J, Rogers N, Hawkesworth C, Harris N, Kelley S, Van Calsteren P, Deng W (1996) Postcollision, shoshonitic volcanism on the Tibetan Plateau: implications for convective thinning of the lithosphere and the source of ocean island basalts. J Petrol 37:45–71

Upton BGJ, Emeleus CH, Heaman LM, Goodenough KM, Finch AA (2003) Magmatism of the mid-Proterozoic Gardar Province,

South Greenland: chronology, petrogenesis and geological setting. Lithos 68:43–65
Wang XM, Zhang RY, Liou JC (1995) UHPM terrane in east central China. In: Coleouan R, Wnag XM (eds) Ultrahigh Pressure Metamorphism. Cambridge University Press, Cambridge, pp 356–390
Wang XX, Wang T, Happala I, Lu XX (2002) Genesis of mafic enclaves from rapakivi-textured granites in the Qinling and its petrological significance: evidence of elements and Nd, Sr isotopes. Acta Petrol Sin 21:935–946 (in Chinese with English abstract)
Wang YM, Gao YS, Han HM, Wang XH (2003) Practical handbook of reference materials for geoanalysis. Geological Publishing House (in Chinese)
Watson EB, Harrison TM (1983) Zircon saturation revisited: temperature and composition effects in a variety of crustal magma types. Earth Planet Sci Lett 64:295–304
Whalen JB, Currie KL, Chappell BW (1987) A-type granites: geochemical characteristics, discrimination and petrogenesis. Contrib Mineral Petrol 95:407–419
Williams HM, Turner SP, Pearce JA, Kelley SP, Harris NBW (2004) Nature of the source regions for post-collisional, potassic magmatism in southern and northern Tibet from geochemical variations and inverse trace element modeling. J Petrol 45:555–607
Xie Z, Li QZ, Gao TS (2006) Comment on "Petrogenesis of post-orogenic syenites in the Sulu orogenic belt, east China: Geochronological, geochemical and Nd-Sr isotopic evidence" by Yang et al. Chem Geol 235:191–194
Yan J, Chen JF, Yu G, Qian H, Zhou TX (2003) Pb isotopic characteristics of Late Mesozoic mafic rocks from the Lower Yangtze Region: evidence for enriched mantle. J China Univ Geosci 9:195–206 (in Chinese)
Yang JH, Chung SL, Wilde SA, Wu FY, Chu MF, Lo CH, Fan HR (2005a) Petrogenesis of post-orogenic syenites in the Sulu Orogenic Belt, East China: geochronological, geochemical and Nd-Sr isotopic evidence. Chem Geol 214:99–125
Yang JH, Wu FY, Chung SL, Wilde SA, Chu MF, Lo CH, Song B (2005b) Petrogenesis of Early Cretaceous intrusions in the Sulu ultrahigh-pressure orogenic belt, east China and their relationship to lithospheric thinning. Chem Geol 222:200–231
Yang K, Wang JP, Lin JZ, Zheng JX, Yang GZ, Ji H (2012) Petrogeochemical characteristics and genetic significance of the Aishan pluton in the Jiaodong Peninsula. Geol Explor 48:693–703
Ye K, Hirajima T, Ishiwateri A (1996) Significance of interstitial coesite in eclogites from Yankou, Qingdao city, eastern China. Chin Sci Bull 41:1047–1048 (in Chinese)
Ye K, Ye DN, Cong BL (2000) The possible subduction of continental material to depths greater than 200 km. Nature 407:734–736
Yuan HL, Gao S, Liu XM, Li HM, Gunther D, Wu FY (2004) Accurate U-Pb age and trace element determinations of zircon by laser ablation-inductively coupled plasma mass spectrometry. Geostand Newslett 28:353–370
Zhai MG, Cong BL, Guo JH, Liu WJ, Li YG, Wang QC (2000) Division of petrological-tectonic units in the northern Sulu ultrahigh-pressure zone: an example of thick-skin thrust of crystalline units. Acta Geol Sin 35:16–26 (in Chinese with English abstract)
Zhang HF, Sun M, Zhou MF, Fan WM, Zhou XH, Zhai MG (2004) Highly heterogeneous Late Mesozoic lithospheric mantle beneath the North China Craton: evidence from Sr-Nd-Pb isotopic systematics of mafic igneous rocks. Geol Mag 141: 55–62
Zhang HF, Sun M, Zhou XH, Ying JF (2005) Geochemical constraints on the origin of Mesozoic alkaline intrusive complexes from the North China Craton and tectonic implications. Lithos 81:297–317
Zhao ZF, Zheng YF (2009) Lithosphere remelting of subducted continent: Mesozoic magmatic petrogenesis of Dabie-Sulu organic belt. Sci China D 39:888–909
Zhao G, Wang D, Cao Q (1997) Geochemical features and petrogenesis of Laoshan Granite in east Shandong Province. Geol J China Univ 3:1–15 (in Chinese with English abstract)
Zheng YF, Fu B, Gong B, Li H (2003) Stable isotope geochemistry of ultrahigh pressure metamorphic rocks from the Dabie-Sulu orogen in China: implications for geodynamics and fluid regime. Earth Sci Rev 62:105–161
Zhong H, Zhu WG, Chu ZY, He DF, Song XY (2007) Shrimp U–Pb zircon geochronology, geochemistry, and Nd–Sr isotopic study of contrasting granites in the Emeishan large igneous province, SW China. Chem Geol 236:112–133
Zhou TH, Lu GX (2000) Tectonics, granitoids and Mesozoic gold deposits in East Shandong, China. Ore Geol Rev 16:71–90
Zhou JB, Zheng YF, Zhao ZF (2003) Zircon U-Pb dating on Mesozoic Granitoids at Wulian, Shandong Province. Geol J China Univ 9:185–194 (in Chinese with English abstract)
Zindler A, Hart SR (1986) Chemical geodynamicas. Annu Earth Planet Sci Lett 14:493–575
Zorpi MJ, Coulon C, Orsini JB (1989) Magma mingling, zoning and emplacement in calc-alkaline granitoid plutons. Tectonophysics 157:315–329
Zou HB, Zindler A, Xu XS, Qi Q (2000) Major, trace element, and Nd, Sr and Pb isotope studies of Cenozoic basalts in SE China: mantle sources, regional variations and tectonic significance. Chem Geol 171:33–47